PROCEEDINGS A

rspa.royalsocietypublishing.org

Research

Cite this article: Nicholls DP. 2018 Stable, high-order computation of impedance–impedance operators for three-dimensional layered medium simulations. *Proc. R. Soc. A* **474**: 20170704. http://dx.doi.org/10.1098/rspa.2017.0704

Received: 6 October 2017
Accepted: 9 March 2018

Subject Areas:
applied mathematics, differential equations, acoustics

Keywords:
impedance–impedance operators, high-order perturbation of surfaces methods, layered media, linear wave scattering, Helmholtz equation, diffraction gratings

Author for correspondence:
David P. Nicholls
e-mail: davidn@uic.edu

Stable, high-order computation of impedance–impedance operators for three-dimensional layered medium simulations

David P. Nicholls

Department of Mathematics, Statistics, and Computer Science, University of Illinois at Chicago, Chicago, IL 60607, USA

DPN, 0000-0002-7424-9832

The faithful modelling of the propagation of linear waves in a layered, periodic structure is of paramount importance in many branches of the applied sciences. In this paper, we present a novel numerical algorithm for the simulation of such problems which is free of the artificial singularities present in related approaches. We advocate for a surface integral formulation which is phrased in terms of impedance–impedance operators that are immune to the Dirichlet eigenvalues which plague the Dirichlet–Neumann operators that appear in classical formulations. We demonstrate a high-order spectral algorithm to simulate these latter operators based upon a high-order perturbation of surfaces methodology which is rapid, robust and highly accurate. We demonstrate the validity and utility of our approach with a sequence of numerical simulations.

1. Introduction

The capability of simulating linear waves interacting with a periodic, layered structure is supremely important in many branches of science and engineering. Examples are easy to find from acoustics (e.g. remote sensing [1], non-destructive testing [2] and underwater acoustics [3]), to electromagnetics (e.g. extraordinary optical transmission [4], surface-enhanced spectroscopy [5] and surface plasmon resonance (SPR) biosensing [6, 7]), to elastodynamics (e.g. full waveform inversion [8] and hazard assessment [9]). In regards to the

THE ROYAL SOCIETY PUBLISHING

SPR phenomena which arise in many areas of nanophotonics [10], due to the strength of the plasmonic effect (the field enhancement can be several orders of magnitude) and its quite sensitive nature (the enhancement is typically only seen over a range of tens of nanometres), such simulations must be very robust and of high accuracy for applications of interest. For this reason, we have a particular interest in high-order spectral (HOS) algorithms [11,12] which deliver high-fidelity solutions with great efficiency.

Engineers and scientists have used all of the classical numerical algorithms for the simulation of this problem (e.g. finite-difference methods [13], finite-element methods [14], discontinuous Galerkin methods [15], spectral element methods [11] and spectral methods [12,16]). But such *volumetric* approaches are greatly disadvantaged with an unnecessarily large number of unknowns for the piecewise homogeneous problems we consider here.

Surface methods can be orders of magnitude faster than the volumetric algorithms discussed above primarily because of the greatly reduced number of degrees of freedom required to resolve a computation, in addition to the *exact* enforcement of far-field boundary conditions. Consequently, these approaches are an extremely important alternative and are becoming more widely used by practitioners. Paramount among these interfacial methods are those based upon integral equations (IEs) [17,18], but these face difficulties. Most have been addressed in recent years through (i) the use of sophisticated quadrature rules to deliver HOS accuracy; (ii) the design of preconditioned iterative solvers with suitable acceleration [19]; and (iii) new strategies to avoid periodizing the Green function [20–27]. Consequently, they are a compelling alternative (see, for example, the survey article of [18] for more details); however, two properties render them non-competitive for the *parametrized* problems we consider compared with the methods we advocate here. (i) For geometries specified by the real value ε (here the deviation of the interface shapes from flat), an IE solver will return the scattering returns only for a particular value of ε. If this value is changed, then the solver must be run again. (ii) The dense, non-symmetric positive definite systems of linear equations which must be inverted with each simulation.

As we advocated in [28,29] a 'high-order perturbation of surfaces' (HOPS) approach can effectively address these concerns. More specifically, we argued for the method of field expansions (FEs), which trace their roots to the low-order calculations of Rayleigh [30] and Rice [31]. The high-order version was first investigated by Bruno & Reitich [32–35] and later enhanced and stabilized by Nicholls & Reitich [36,37] with the method of transformed field expansions (TFEs). These formulations maintain the advantageous properties of classical IE formulations (e.g. surface formulation and exact enforcement of far-field conditions) while avoiding the shortcomings listed above: (i) as HOPS methods are built upon expansions in the deformation parameter, ε, once the Taylor coefficients are known for the scattering quantities, it is simply a matter of summing these (rather than beginning a new simulation) for any given choice of ε to recover the returns; (ii) due to the perturbative nature of the scheme, at every Taylor order one need only invert a single, sparse operator corresponding to the flat-interface, order-zero approximation of the problem.

Regardless of the strategy employed, the precise formulation of the problem can strongly influence the performance of any of these numerical methods. Of particular note, when there are internal layers present in the structure, a wise formulation will avoid the 'Dirichlet eigenvalues' present for such domains. In short, if Dirichlet traces are used as data at these interfaces, 'artificial' singularities can be introduced which are not exhibited by the full, coupled system. More specifically, many formulations use Dirichlet–Neumann operators (DNOs) (e.g. [38,39]) when it is a trivial matter to *explicitly* compute layer thicknesses where the underlying Dirichlet problem delivers a non-unique solution. One approach to eliminating this artificial source of singularity is to employ a domain decomposition method (DDM), first described for Laplace's equation by Lions [40] and adapted to the Helmholtz problem by Després [41,42] (see the survey article of Collino *et al*. [43] for more details). For this one matches 'conjugate' impedances (Robin data) of the solution at layer interfaces, and, in the present context, we employ 'impedance–impedance operators' (IIOs) to map one to the other as advocated by Collino *et al*. [43] (see also Gillman *et al*. [38]). On interior layers these IIOs are unitary so that not only are their eigenvalues non-zero,

but also they are restricted to the unit circle in the complex plane, giving, as we shall see, a very well-conditioned algorithm.

In this contribution, we will discuss a novel, rapid, stable and HOS method for the simulation of IIOs which arise in layered medium configurations. Furthermore, we will demonstrate these properties through a sequence of numerical simulations compared with similar calculations for DNOs at, and near, their Dirichlet eigenvalues. We conclude with the simulation of a triply layered configuration which arises in the study of SPR biosensors featuring *corrugated* interfaces between a dielectric and a metal [29,44]. While the TFE recursions we describe here have been used to simulate DNOs on unbounded domains, they have not been implemented on interior layers mainly because of the problems created by the Dirichlet eigenvalues. Furthermore, IIOs have never been simulated using this TFE algorithm, so there are many new details contained herein which allow one to simulate configurations which, until now, were inaccessible to HOPS algorithms.

The rest of the paper is organized as follows. In §2, we recall the governing equations for scattering of linear waves by a periodic layered medium in three dimensions, with a particular discussion of transparent boundary conditions. In §3, we describe an interfacial reformulation of these equations in terms of surface quantities and IIOs that generalizes our previous formulation [39,45]. In §4, we begin a detailed discussion of these IIOs by explicitly computing their action on domains with infinitesimal (flat) interfaces. In §5, we describe our stable, HOS HOPS scheme for simulating solutions of our new formulation: the TFE method. In §6, we display our numerical results with implementation details, with validation of our implementation provided in §6a and results for a triply layered structure in §6b.

2. Governing equations

The Helmholtz equation governs the scattering of linear acoustic waves in a periodic layered structure, with insonification conditions at the upper interface, and upward and downward propagating wave conditions at positive and negative infinities [46,47]. For the latter of these, we demand the 'upward propagating Rayleigh expansion radiation condition' (URC) and its 'downward propagating' analogue (DRC) as specified in [48] (which we make precise in §2). In [45], we detailed a restatement of the classical governing equations in terms of DNOs, which we revise in this contribution (see §3).

We consider a multiply layered material with M many $d_x \times d_y$ periodic interfaces at

$$z = a^{(m)} + g^{(m)}(x,y), \quad g^{(m)}(x+d_x, y+d_y) = g^{(m)}(x,y), \quad 1 \le m \le M,$$

separating $(M+1)$-many layers which define the domains

$$S^{(0)} := \{(x,y,z) \,|\, z > a^{(1)} + g^{(1)}(x,y)\},$$
$$S^{(m)} := \{(x,y,z) \,|\, a^{(m+1)} + g^{(m+1)}(x,y) < z < a^{(m)} + g^{(m)}(x,y)\}, \quad 1 \le m \le M-1$$

and
$$S^{(M)} := \{(x,y,z) \,|\, z < a^{(M)} + g^{(M)}(x,y)\},$$

with (upward pointing) normals $N^{(m)} := (-\partial_x g^{(m)}(x,y), -\partial_y g^{(m)}(x,y), 1)^{\mathrm{T}}$ (figure 1). The $(M+1)$ domains are all lossless, constant-density acoustic media with velocities $c^{(m)}$ $(m = 0, \ldots, M)$ and we assume that plane-wave radiation is incident upon the structure from above

$$\underline{v}^{\mathrm{inc}}(x,y,z,t) = \mathrm{e}^{-\mathrm{i}\omega t}\,\mathrm{e}^{\mathrm{i}(\alpha x + \beta y - \gamma^{(0)} z)} = \mathrm{e}^{-\mathrm{i}\omega t} v^{\mathrm{inc}}(x,y,z).$$

In each layer, the parameter $k^{(m)} = \omega / c^{(m)}$ characterizes both the properties of the material and the frequency of radiation in the structure. We denote the reduced scattered fields in $S^{(m)}$ by

$$v^{(m)}(x,y,z) = \mathrm{e}^{\mathrm{i}\omega t} \underline{v}^{(m)}(x,y,z,t)$$

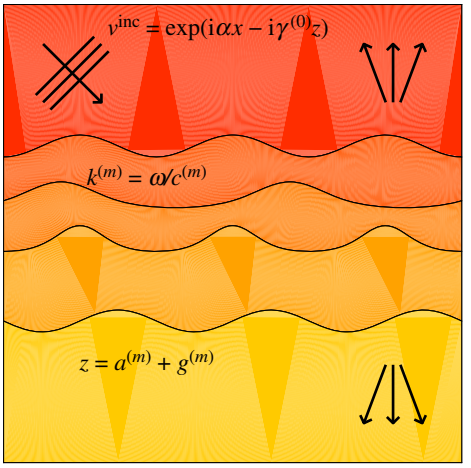

Figure 1. Five-layer problem configuration with layer interfaces $z = a^{(m)} + g^{(m)}(x)$. (Online version in colour.)

(the full scattered fields with the periodic time dependence factored out), which, like the incident radiation, will be quasi-periodic [47]

$$v^{(m)}(x + d_x, y + d_y, z) = \mathrm{e}^{\mathrm{i}(\alpha d_x + \beta d_y)} v^{(m)}(x, y, z), \quad m = 0, \ldots, M.$$

These reduced fields satisfy the Helmholtz equations

$$\Delta v^{(m)} + (k^{(m)})^2 v^{(m)} = 0, \quad \text{in } S^{(m)}, \quad 0 \le m \le M, \tag{2.1}$$

which are coupled through the Dirichlet and Neumann boundary conditions

$$v^{(m-1)} - v^{(m)} = \zeta^{(m)}, \quad z = a^{(m)} + g^{(m)}(x, y), \quad 1 \le m \le M \tag{2.2a}$$

and

$$\left.\begin{aligned} &\partial_{N^{(m)}} v^{(m-1)} - (\tau^{(m)})^2 \partial_{N^{(m)}} v^{(m)} = \psi^{(m)} \\ \text{and} \quad &z = a^{(m)} + g^{(m)}(x, y), \quad 1 \le m \le M, \end{aligned}\right\} \tag{2.2b}$$

where $\tau^{(m)} = 1$ in transverse electric (TE) polarization, $\tau^{(m)} = k^{(m-1)}/k^{(m)}$ in transverse magnetic (TM) polarization and

$$\begin{aligned} &\zeta^{(1)}(x, y) := -v^{\mathrm{inc}}(x, y, a^{(1)} + g^{(1)}(x, y)) = -\mathrm{e}^{\mathrm{i}(\alpha x + \beta y - \gamma^{(0)}(a^{(1)} + g^{(1)}(x,y)))} \\ \text{and} \quad &\psi^{(1)}(x, y) := -[\partial_{N^{(1)}} v^{\mathrm{inc}}(x, y, z)]_{z = a^{(1)} + g^{(1)}(x,y)} \\ &\qquad = (\mathrm{i}\gamma^{(0)} + \mathrm{i}\alpha(\partial_x g^{(1)}) + \mathrm{i}\beta(\partial_y g^{(1)}))\, \mathrm{e}^{\mathrm{i}(\alpha x + \beta y - \gamma^{(0)}(a^{(1)} + g^{(1)}(x,y)))}. \end{aligned}$$

If continuity is enforced inside the structure, then $\zeta^{(m)} \equiv \psi^{(m)} \equiv 0$, $m = 2, \ldots, M$. However, as we shall see, it is no impediment to the method if we set these to any non-zero function.

Regarding the upward/downward propagating wave conditions (URC/DRC), we introduce the planes

$$z = \overline{a} > a^{(1)} + \left|g^{(1)}\right|_{L^\infty} \quad \text{and} \quad z = \underline{a} < a^{(M)} - \left|g^{(M)}\right|_{L^\infty},$$

define the domains $\overline{S} := \{z > \overline{a}\}$ and $\underline{S} := \{z < \underline{a}\}$, and note that we can find unique quasi-periodic solutions of the relevant Helmholtz problems on each of these domains given generic Dirichlet data, say $\xi(x,y)$ and $\mu(x,y)$. For this, we use the Rayleigh expansions [30], which state that

$$v^{(0)}(x,y,z) = \sum_{p=-\infty}^{\infty}\sum_{q=-\infty}^{\infty} \hat{\xi}_{p,q}\, \mathrm{e}^{\mathrm{i}\alpha_p x + \mathrm{i}\beta_q y + \mathrm{i}\gamma_{p,q}^{(0)}(z-\overline{a})}, \quad \text{in } \overline{S}$$

$$\text{and} \quad v^{(M)}(x,y,z) = \sum_{p=-\infty}^{\infty}\sum_{q=-\infty}^{\infty} \hat{\mu}_{p,q}\, \mathrm{e}^{\mathrm{i}\alpha_p x + \mathrm{i}\beta_q y - \mathrm{i}\gamma_{p,q}^{(M)}(z-\underline{a})}, \quad \text{in } \underline{S},$$

where

$$\hat{\xi}_{p,q} = \frac{1}{d_x d_y}\int_0^{d_x}\int_0^{d_y} \xi(x,y)\, \mathrm{e}^{-\mathrm{i}\alpha_p x - \mathrm{i}\beta_q y}\, \mathrm{d}x\, \mathrm{d}y,$$

for $p, q \in \mathbf{Z}$, $m \in \{0, \ldots, M\}$,

$$\alpha_p := \alpha + \left(\frac{2\pi}{d_x}\right)p, \quad \beta_q := \beta + \left(\frac{2\pi}{d_y}\right)q$$

$$\text{and} \quad \gamma_{p,q}^{(m)} := \begin{cases} \sqrt{(k^{(m)})^2 - \alpha_p^2 - \beta_q^2}, & (p,q) \in \mathcal{U}^{(m)}, \\ \mathrm{i}\sqrt{\alpha_p^2 + \beta_q^2 - (k^{(m)})^2}, & (p,q) \notin \mathcal{U}^{(m)}, \end{cases}$$

and the set of propagating modes is

$$\mathcal{U}^{(m)} := \{(p,q) \in \mathbf{Z} \,|\, \alpha_p^2 + \beta_q^2 \leq (k^{(m)})^2\}.$$

We note that

$$v^{(0)}(x,y,\overline{a}) = \sum_{p=-\infty}^{\infty}\sum_{q=-\infty}^{\infty} \hat{\xi}_{p,q}\, \mathrm{e}^{\mathrm{i}\alpha_p x + i\beta_q y} = \xi(x,y)$$

$$\text{and} \quad v^{(M)}(x,y,\underline{a}) = \sum_{p=-\infty}^{\infty}\sum_{q=-\infty}^{\infty} \hat{\mu}_{p,q}\, \mathrm{e}^{\mathrm{i}\alpha_p x + i\beta_q y} = \mu(x,y).$$

With these formulae, we can compute the *outward-pointing* Neumann data at the artificial boundaries

$$-\partial_z v^{(0)}(x,y,\overline{a}) = \sum_{p=-\infty}^{\infty}\sum_{q=-\infty}^{\infty} -(\mathrm{i}\gamma_{p,q}^{(0)})\hat{\xi}_{p,q}\, \mathrm{e}^{\mathrm{i}\alpha_p x + \mathrm{i}\beta_q y} =: T^{(0)}[\xi(x,y)]$$

$$\text{and} \quad \partial_z v^{(M)}(x,y,\underline{a}) = \sum_{p=-\infty}^{\infty}\sum_{q=-\infty}^{\infty} (-\mathrm{i}\gamma_{p,q}^{(M)})\hat{\mu}_{p,q}\, \mathrm{e}^{\mathrm{i}\alpha_p x + \mathrm{i}\beta_q y} =: T^{(M)}[\mu(x,y)],$$

which define the Fourier multipliers, $\{T^{(0)}, T^{(M)}\}$.

With these operators, it is not difficult to see that quasi-periodic, upward propagating solutions to the Helmholtz equation (2.1) with $m = 0$ equivalently solve

$$\Delta v^{(0)} + (k^{(0)})^2 v^{(0)} = 0, \quad a^{(1)} + g^{(1)}(x,y) < z < \overline{a} \tag{2.3a}$$

and

$$\partial_z v^{(0)} + T^{(0)}[v^{(0)}] = 0, \quad z = \overline{a}. \tag{2.3b}$$

Similarly, one can show that quasi-periodic, downward propagating solutions to the Helmholtz equation (2.1) with $m = M$ equivalently solve

$$\Delta v^{(M)} + (k^{(M)})^2 v^{(M)} = 0, \quad \underline{a} < z < a^{(M)} + g^{(M)}(x,y) \tag{2.4a}$$

and

$$\partial_z v^{(M)} - T^{(M)}[v^{(M)}] = 0, \quad z = \underline{a}. \tag{2.4b}$$

Remark 2.1. We point out that conditions (2.3*b*) and (2.4*b*) specify solutions which satisfy the UPC and DPC of definition 2.6 in Arens [48]. It is these two conditions which guarantee the uniqueness of solutions on the unbounded domains $\{z > \overline{a}\}$ and $\{z < \underline{a}\}$.

3. Boundary formulation: impedance–impedance operators

While extremely useful for many configurations of interest, our previous formulation of the scattering problem above [39,45] in terms of surface operators suffers from the fact that interior layer DNOs, H, do not exist at the 'Dirichlet eigenvalues', i.e. choices of $k^{(m)}$ for which (2.1) does not have a unique solution. To fix this, we follow the lead of Kirsch & Monk [49] and Gillman *et al*. [38] by pursuing IIOs which exist at all values of $k^{(m)}$.

To begin we consider a positive, non-zero constant $\eta \in \mathbf{R}^+$ and reduce our set of unknowns to the following surface quantities:

$$U^{(m),\ell}(x,y) := -\partial_{N^{(m+1)}} v^{(m)} - \mathrm{i}\eta v^{(m)}, \quad z = a^{(m+1)} + g^{(m+1)}, \quad 0 \le m \le M-1,$$
$$U^{(m),u}(x,y) := \partial_{N^{(m)}} v^{(m)} - \mathrm{i}\eta v^{(m)}, \quad z = a^{(m)} + g^{(m)}, \quad 1 \le m \le M,$$
$$\tilde{U}^{(m),\ell}(x,y) := -\partial_{N^{(m+1)}} v^{(m)} + \mathrm{i}\eta v^{(m)}, \quad z = a^{(m+1)} + g^{(m+1)}, \quad 0 \le m \le M-1$$

and
$$\tilde{U}^{(m),u}(x,y) := \partial_{N^{(m)}} v^{(m)} + \mathrm{i}\eta v^{(m)}, \quad z = a^{(m)} + g^{(m)}, \quad 1 \le m \le M.$$

Using the fact that, from these, one could recover the scattered field at any point with a suitable integral formula [50], we find that our governing equations reduce to the boundary conditions (2.2*a*), which we express as

$$U^{(m-1),\ell} - \tilde{U}^{(m-1),\ell} - U^{(m),u} + \tilde{U}^{(m),u} = -2\mathrm{i}\eta\zeta^{(m)}, \quad 1 \le m \le M \tag{3.1a}$$

and
$$U^{(m-1),\ell} + \tilde{U}^{(m-1),\ell} + (\tau^{(m)})^2 U^{(m),u} + (\tau^{(m)})^2 \tilde{U}^{(m),u} = -2\psi^{(m)}, \quad 1 \le m \le M. \tag{3.1b}$$

We can further simplify by introducing IIOs, and for this we make the following definitions.

Definition 3.1. Given a sufficiently smooth deformation $g^{(1)}(x,y)$, the unique quasi-periodic solution of

$$\Delta v^{(0)} + (k^{(0)})^2 v^{(0)} = 0, \quad a^{(1)} + g^{(1)}(x,y) < z < \overline{a}, \tag{3.2a}$$
$$\partial_z v^{(0)} + T^{(0)}[v^{(0)}] = 0, \quad z = \overline{a} \tag{3.2b}$$

and
$$-\partial_{N^{(1)}} v^{(0)} - \mathrm{i}\eta v^{(0)} = U^{(0),\ell}, \quad z = a^{(1)} + g^{(1)}(x,y) \tag{3.2c}$$

defines the IIO

$$Q[U^{(0),\ell}] = Q(\overline{a}, a^{(1)}, g^{(1)})[U^{(0),\ell}] := \tilde{U}^{(0),\ell}. \tag{3.3}$$

Definition 3.2. Given sufficiently smooth deformations $g^{(m)}(x,y)$ and $g^{(m+1)}(x,y)$, for $1 \le m \le M-1$, the unique quasi-periodic solution of

$$\Delta v^{(m)} + (k^{(m)})^2 v^{(m)} = 0, \quad a^{(m+1)} + g^{(m+1)}(x,y) < z < a^{(m)} + g^{(m)}(x,y), \tag{3.4a}$$
$$\partial_{N^{(m)}} v^{(m)} - \mathrm{i}\eta v^{(m)} = U^{(m),u}, \quad z = a^{(m)} + g^{(m)}(x,y) \tag{3.4b}$$

and
$$-\partial_{N^{(m+1)}} v^{(m)} - \mathrm{i}\eta v^{(m)} = U^{(m),\ell}, \quad z = a^{(m+1)} + g^{(m+1)}(x,y) \tag{3.4c}$$

defines the IIO

$$R(m)\left[\begin{pmatrix} U^{(m),u} \\ U^{(m),\ell} \end{pmatrix}\right] = R(m; a^{(m)}, g^{(m)}, a^{(m+1)}, g^{(m+1)})\left[\begin{pmatrix} U^{(m),u} \\ U^{(m),\ell} \end{pmatrix}\right]$$
$$= \begin{pmatrix} R^{uu}(m) & R^{u\ell}(m) \\ R^{\ell u}(m) & R^{\ell\ell}(m) \end{pmatrix}\left[\begin{pmatrix} U^{(m),u} \\ U^{(m),\ell} \end{pmatrix}\right] := \begin{pmatrix} \tilde{U}^{(m),u} \\ \tilde{U}^{(m),\ell} \end{pmatrix}. \tag{3.5}$$

Definition 3.3. Given a sufficiently smooth deformation $g^{(M)}(x,y)$, the unique quasi-periodic solution of

$$\Delta v^{(M)} + (k^{(M)})^2 v^{(M)} = 0, \quad \underline{a} < z < a^{(M)} + g^{(M)}(x,y), \tag{3.6a}$$

$$\partial_{N^{(M)}} v^{(M)} - \mathrm{i}\eta v^{(M)} = U^{(M),u}, \quad z = a^{(M)} + g^{(M)}(x,y) \tag{3.6b}$$

and

$$\partial_z v^{(M)} - T^{(M)}[v^{(M)}] = 0, \quad z = \underline{a} \tag{3.6c}$$

defines the IIO

$$S[U^{(M),u}] = S(\underline{a}, a^{(M)}, g^{(M)})[U^{(M),u}] := \tilde{U}^{(M),u}. \tag{3.7}$$

Remark 3.4. Using the approach in [39], it is possible to show that $g^{(m)} \in C^{s+3/2+\sigma}([0,d_x] \times [0,d_y])$ for any integer $s \geq 0$, and any real $\sigma > 0$ is smooth enough to define Q, R and S. In fact, with a more subtle analysis, Lipschitz smooth will also suffice [51,52].

In terms of this notation, the boundary conditions (3.1) become

$$\begin{aligned}
&\{I - Q\}[U^{(0),\ell}] + \{-I + R^{uu}(1)\}[U^{(1),u}] + R^{u\ell}(1)[U^{(1),\ell}] = -2\mathrm{i}\eta\zeta^{(1)},\\
&-R^{\ell u}(m-1)[U^{(m-1),u}] + \{I - R^{\ell\ell}(m-1)\}[U^{(m-1),\ell}]\\
&\quad + \{-I + R^{uu}(m)\}[U^{(m),u}] + R^{u\ell}(m)[U^{(m),\ell}] = -2\mathrm{i}\eta\zeta^{(m)}, \quad 2 \leq m \leq M-1,\\
&-R^{\ell u}(M-1)[U^{(M-1),u}] + \{I - R^{\ell\ell}(M-1)\}[U^{(M-1),\ell}]\\
&\quad + \{-I + S\}[U^{(M),u}] = -2\mathrm{i}\eta\zeta^{(M)}
\end{aligned}$$

and

$$\begin{aligned}
&\{I + Q\}[U^{(0),\ell}] + (\tau^{(1)})^2\{I + R^{uu}(1)\}[U^{(1),u}]\\
&\quad + (\tau^{(1)})^2 R^{u\ell}(1)[U^{(1),\ell}] = -2\psi^{(1)},\\
&R^{\ell u}(m-1)[U^{(m-1),u}] + \{I + R^{\ell\ell}(m-1)\}[U^{(m-1),\ell}] + (\tau^{(m)})^2\{I\\
&\quad + R^{uu}(m)\}[U^{(m),u}] + (\tau^{(m)})^2 R^{u\ell}(m)[U^{(m),\ell}] = -2\psi^{(m)}, \quad 2 \leq m \leq M-1,\\
&R^{\ell u}(M-1)[U^{(M-1),u}] + \{I + R^{\ell\ell}(M-1)\}[U^{(M-1),\ell}]\\
&\quad + (\tau^{(M)})^2\{I + S\}[U^{(M),u}] = -2\psi^{(M)}.
\end{aligned}$$

We write this more compactly as

$$(\mathbf{L} + \mathbf{D} + \mathbf{U})\mathbf{x} = \mathbf{A}\mathbf{x} = \mathbf{b}, \tag{3.8}$$

where

$$\mathbf{x} := (U^{(0),\ell} \quad U^{(1),u} \quad U^{(1),\ell} \quad \cdots \quad U^{(M-1),u} \quad U^{(M-1),\ell} \quad U^{(M),u})^{\mathrm{T}},$$

$$\mathbf{b} := -2((\mathrm{i}\eta)\zeta^{(1)} \quad \psi^{(1)} \quad \cdots \quad (\mathrm{i}\eta)\zeta^{(M)} \quad \psi^{(M)})^{\mathrm{T}},$$

$$\mathbf{A} = \begin{pmatrix}
\mathbf{D}(1) & \mathbf{U}(1) & 0 & 0 & \cdots & 0\\
\mathbf{L}(2) & \mathbf{D}(2) & \mathbf{U}(2) & 0 & \cdots & 0\\
0 & \ddots & \ddots & \ddots & 0 & 0\\
0 & 0 & \ddots & \ddots & \ddots & 0\\
0 & \cdots & 0 & \mathbf{L}(M-1) & \mathbf{D}(M-1) & \mathbf{U}(M-1)\\
0 & \cdots & 0 & 0 & \mathbf{L}(M) & \mathbf{D}(M)
\end{pmatrix}$$

and

$$\mathbf{U}(m)=\begin{pmatrix} R^{u\ell}(m) & 0\\ (\tau^{(m)})^2R^{u\ell}(m) & 0\end{pmatrix},\quad 1\le m\le M-1,$$

$$\mathbf{L}(m)=\begin{pmatrix} 0 & -R^{\ell u}(m)\\ 0 & R^{\ell u}(m)\end{pmatrix},\quad 2\le m\le M,$$

$$\mathbf{D}(1)=\begin{pmatrix} I-Q & -I+R^{uu}(1)\\ I+Q & (\tau^{(1)})^2(I+R^{uu}(1))\end{pmatrix},$$

$$\mathbf{D}(m)=\begin{pmatrix} I-R^{\ell\ell}(m-1) & -I+R^{uu}(m)\\ I+R^{\ell\ell}(m-1) & (\tau^{(m)})^2(I+R^{uu}(m))\end{pmatrix},\quad 2\le m\le M-1,$$

$$\mathbf{D}(M)=\begin{pmatrix} I-R^{\ell\ell}(M-1) & -I+S\\ I+R^{\ell\ell}(M-1) & (\tau^{(M)})^2(I+S)\end{pmatrix}.$$

4. Impedance–impedance operators: infinitesimal interfaces

We can gain insight into these IIOs by studying them in the case of *infinitesimal* grating interfaces, which we model by quasi-periodic solutions in the case $g^{(m)}\equiv 0$. We begin with the upper layer, where it is easy to see that the solution of (3.2*a*,*b*) is

$$v^{(0)}(x,y,z)=\sum_{p=-\infty}^{\infty}\sum_{q=-\infty}^{\infty}a_{p,q}\,\mathrm{e}^{\mathrm{i}\alpha_p x+\mathrm{i}\beta_q y+\mathrm{i}\gamma_{p,q}^{(0)}(z-a^{(1)})}.$$

The boundary condition (3.2*c*) demands that

$$\widehat{U^{(0),\ell}}_{p,q}=a_{p,q}(-\mathrm{i}\gamma_{p,q}^{(0)}-\mathrm{i}\eta),$$

giving

$$v^{(0)}(x,y,z)=\sum_{p=-\infty}^{\infty}\sum_{q=-\infty}^{\infty}\frac{\widehat{U^{(0),\ell}}_{p,q}}{(-\mathrm{i}\gamma_{p,q}^{(0)}-\mathrm{i}\eta)}\,\mathrm{e}^{\mathrm{i}\alpha_p x+\mathrm{i}\beta_q y+\mathrm{i}\gamma_{p,q}^{(0)}(z-a^{(1)})},$$

which is well defined since $(-\mathrm{i}\gamma_{p,q}^{(0)}-\mathrm{i}\eta)\neq 0$ provided that $\eta>0$. Thus,

$$\begin{aligned}Q(0)[U^{(0),\ell}]&=-\partial_z v^{(0)}(x,y,a^{(1)})+\mathrm{i}\eta v^{(0)}(x,y,a^{(1)})\\&=\sum_{p=-\infty}^{\infty}\sum_{q=-\infty}^{\infty}\frac{(-\mathrm{i}\gamma_{p,q}^{(0)}+\mathrm{i}\eta)}{(-\mathrm{i}\gamma_{p,q}^{(0)}-\mathrm{i}\eta)}\widehat{U^{(0),\ell}}_{p,q}\,\mathrm{e}^{\mathrm{i}\alpha_p x+\mathrm{i}\beta_q y},\end{aligned}$$

which gives the order-zero Fourier multiplier

$$Q(0)=\left(\frac{-\mathrm{i}\gamma_D^{(0)}+\mathrm{i}\eta}{-\mathrm{i}\gamma_D^{(0)}-\mathrm{i}\eta}\right).$$

In a similar manner, it can be shown that

$$S(0)=\left(\frac{-\mathrm{i}\gamma_D^{(M)}+\mathrm{i}\eta}{-\mathrm{i}\gamma_D^{(M)}-\mathrm{i}\eta}\right).$$

We close with the inner layer case where we observe that, if we map $\{a^{(m+1)}<z<a^{(m)}\}$ to $\{-\bar{h}^{(m)}<z<\bar{h}^{(m)}\}$ where

$$\bar{h}^{(m)}:=\frac{(a^{(m)}-a^{(m+1)})}{2},\quad 1\le m\le M-1,$$

the solution of (3.4*a*) is

$$v^{(m)}(x,y,z)=\sum_{p=-\infty}^{\infty}\sum_{q=-\infty}^{\infty}\left\{B_{p,q}\cosh(\mathrm{i}\gamma_{p,q}^{(m)}z)+C_{p,q}\frac{\sinh(\mathrm{i}\gamma_{p,q}^{(m)}z)}{(\mathrm{i}\gamma_{p,q}^{(m)})}\right\}\mathrm{e}^{\mathrm{i}\alpha_p x+\mathrm{i}\beta_q y},$$

where

$$\cosh(\mathrm{i}\gamma_{p,q}^{(m)}z):=\begin{cases}\cos(\gamma_{p,q}^{(m)}z), & (p,q)\in\mathcal{U}^{(m)} \implies \mathrm{Im}\{\gamma_{p,q}^{(m)}\}=0,\\ 1, & \gamma_{p,q}^{(m)}=0,\\ \cosh(\mathrm{Im}\{\gamma_{p,q}^{(m)}\}z), & (p,q)\notin\mathcal{U}^{(m)} \implies \mathrm{Re}\{\gamma_{p,q}^{(m)}\}=0,\end{cases}$$

and

$$\frac{\sinh(\mathrm{i}\gamma_{p,q}^{(m)}z)}{(\mathrm{i}\gamma_{p,q}^{(m)})}:=\begin{cases}\dfrac{\sin(\gamma_{p,q}^{(m)}z)}{\gamma_{p,q}^{(m)}}, & (p,q)\in\mathcal{U}^{(m)} \implies \mathrm{Im}\{\gamma_{p,q}^{(m)}\}=0,\\ z, & \gamma_{p,q}^{(m)}=0,\\ \dfrac{\sinh(\mathrm{Im}\{\gamma_{p,q}^{(m)}\}z)}{\mathrm{Im}\{\gamma_{p,q}^{(m)}\}}, & (p,q)\notin\mathcal{U}^{(m)} \implies \mathrm{Re}\{\gamma_{p,q}^{(m)}\}=0.\end{cases}$$

Using the facts that

$$d_z[\cosh(\mathrm{i}\gamma_{p,q}^{(m)}z)]=(\mathrm{i}\gamma_{p,q}^{(m)})^2\frac{\sinh(\mathrm{i}\gamma_{p,q}^{(m)}z)}{\mathrm{i}\gamma_{p,q}^{(m)}} \quad\text{and}\quad d_z\left[\frac{\sinh(\mathrm{i}\gamma_{p,q}^{(m)}z)}{\mathrm{i}\gamma_{p,q}^{(m)}}\right]=\cosh(\mathrm{i}\gamma_{p,q}^{(m)}z),$$

and the oddness of sinh, boundary conditions (3.4*b*,*c*) demand that

$$\widehat{U^{(m),u}}_{p,q}=B_{p,q}(\mathrm{i}\gamma_{p,q}^{(m)})^2\mathrm{sh}_{p,q}+C_{p,q}\mathrm{ch}_{p,q}-(\mathrm{i}\eta)\{B_{p,q}\mathrm{ch}_{p,q}+C_{p,q}\mathrm{sh}_{p,q}\}$$

and

$$\widehat{U^{(m),\ell}}_{p,q}=B_{p,q}(\mathrm{i}\gamma_{p,q}^{(m)})^2\mathrm{sh}_{p,q}-C_{p,q}\mathrm{ch}_{p,q}-(\mathrm{i}\eta)\{B_{p,q}\mathrm{ch}_{p,q}-C_{p,q}\mathrm{sh}_{p,q}\},$$

where

$$\mathrm{ch}_{p,q}:=\cosh(\mathrm{i}\gamma_{p,q}\bar{h}^{(m)})=\begin{cases}\cos(\gamma_{p,q}^{(m)}\bar{h}^{(m)}), & (p,q)\in\mathcal{U}^{(m)},\\ 1, & \gamma_{p,q}^{(m)}=0,\\ \cosh(\mathrm{Im}\{\gamma_{p,q}^{(m)}\}\bar{h}^{(m)}), & (p,q)\notin\mathcal{U}^{(m)},\end{cases}$$

$$\mathrm{sh}_{p,q}:=\frac{\sinh(\mathrm{i}\gamma_{p,q}^{(m)}\bar{h}^{(m)})}{(\mathrm{i}\gamma_{p,q}^{(m)})}=\begin{cases}\dfrac{\sin(\gamma_{p,q}^{(m)}\bar{h}^{(m)})}{\gamma_{p,q}^{(m)}}, & (p,q)\in\mathcal{U}^{(m)},\\ \bar{h}^{(m)}, & \gamma_{p,q}^{(m)}=0,\\ \dfrac{\sinh(\mathrm{Im}\{\gamma_{p,q}^{(m)}\}\bar{h}^{(m)})}{\mathrm{Im}\{\gamma_{p,q}^{(m)}\}}, & (p,q)\notin\mathcal{U}^{(m)}\end{cases}$$

or

$$\begin{pmatrix}-(\gamma_{p,q}^{(m)})^2\mathrm{sh}_{p,q}-(\mathrm{i}\eta)\mathrm{ch}_{p,q} & \mathrm{ch}_{p,q}-(\mathrm{i}\eta)\mathrm{sh}_{p,q}\\ -(\gamma_{p,q}^{(m)})^2\mathrm{sh}_{p,q}-(\mathrm{i}\eta)\mathrm{ch}_{p,q} & -\mathrm{ch}_{p,q}+(\mathrm{i}\eta)\mathrm{sh}_{p,q}\end{pmatrix}\begin{pmatrix}B_{p,q}\\ C_{p,q}\end{pmatrix}=\begin{pmatrix}\widehat{U^{(m),u}}_{p,q}\\ \widehat{U^{(m),\ell}}_{p,q}\end{pmatrix}.$$

To simplify the notation, we define

$$a:=-(\gamma_{p,q}^{(m)})^2\mathrm{sh}_{p,q}-(\mathrm{i}\eta)\mathrm{ch}_{p,q} \quad\text{and}\quad b:=\mathrm{ch}_{p,q}-(\mathrm{i}\eta)\mathrm{sh}_{p,q},$$

which delivers

$$\begin{pmatrix} a & b \\ a & -b \end{pmatrix} \begin{pmatrix} B_{p,q} \\ C_{p,q} \end{pmatrix} = \begin{pmatrix} \widehat{U^{(m),u}}_{p,q} \\ \widehat{U^{(m),\ell}}_{p,q} \end{pmatrix}.$$

As the determinant of the matrix on the left-hand side

$$\begin{aligned} -2ab &= -2\{-(\gamma_{p,q}^{(m)})^2 \mathrm{sh}_{p,q} - (\mathrm{i}\eta)\mathrm{ch}_{p,q}\}\{\mathrm{ch}_{p,q} - (\mathrm{i}\eta)\mathrm{sh}_{p,q}\} \\ &= 2((\gamma_{p,q}^{(m)})^2 + \eta^2)\mathrm{sh}_{p,q}\mathrm{ch}_{p,q} + 2(\mathrm{i}\eta)(\mathrm{ch}_{p,q}^2 - (\gamma_{p,q}^{(m)})^2 \mathrm{sh}_{p,q}^2) \end{aligned}$$

is never zero, we find the unique solution

$$\begin{pmatrix} B_{p,q} \\ C_{p,q} \end{pmatrix} = \frac{1}{2} \begin{pmatrix} \frac{1}{a} & \frac{1}{a} \\ \frac{1}{b} & -\frac{1}{b} \end{pmatrix} \begin{pmatrix} \widehat{U^{(m),u}}_{p,q} \\ \widehat{U^{(m),\ell}}_{p,q} \end{pmatrix}.$$

Using these, we can compute the IIO

$$\begin{aligned} \begin{pmatrix} \widehat{\tilde{U}^{(m),u}}_{p,q} \\ \widehat{\tilde{U}^{(m),\ell}}_{p,q} \end{pmatrix} &= \begin{pmatrix} [\partial_z v + (\mathrm{i}\eta)v]_{z=h} \\ [-\partial_z v + (\mathrm{i}\eta)v]_{z=-h} \end{pmatrix} = \begin{pmatrix} \bar{a} & \bar{b} \\ \bar{a} & -\bar{b} \end{pmatrix} \begin{pmatrix} B_{p,q} \\ C_{p,q} \end{pmatrix} \\ &= \begin{pmatrix} \bar{a} & \bar{b} \\ \bar{a} & -\bar{b} \end{pmatrix} \frac{1}{2} \begin{pmatrix} \frac{1}{a} & \frac{1}{a} \\ \frac{1}{b} & -\frac{1}{b} \end{pmatrix} \begin{pmatrix} \widehat{U^{(m),u}}_{p,q} \\ \widehat{U^{(m),\ell}}_{p,q} \end{pmatrix} = R_0 \begin{pmatrix} \widehat{U^{(m),u}}_{p,q} \\ \widehat{U^{(m),\ell}}_{p,q} \end{pmatrix}, \end{aligned}$$

where

$$R_0 = \frac{1}{2} \begin{pmatrix} \frac{\bar{a}}{a} + \frac{\bar{b}}{b} & \frac{\bar{a}}{a} - \frac{\bar{b}}{b} \\ \frac{\bar{a}}{a} - \frac{\bar{b}}{b} & \frac{\bar{a}}{a} + \frac{\bar{b}}{b} \end{pmatrix}.$$

It is not difficult to show that R_0 is unitary, i.e. $R_0^{-1} = R_0^*$, from the fact that $|\bar{a}/a| = \left|\bar{b}/b\right| = 1$. Beyond this, it can be shown that R is unitary even when $g^{(m)} \not\equiv 0$ [38].

5. The method of transformed field expansions

We now show how a stable, high-order numerical implementation of (3.8) can deliver high-quality simulations of layered medium configurations. For this, we need to describe a method for simulating the IIOs, Q, $R(m)$ and S. Up to this point, our developments have been neutral on this topic: any of the methods we described in the Introduction, from finite differences to IEs, could be used to approximate solutions of (3.2), (3.4) and (3.6). However, as we argued there, volumetric methods are needlessly disadvantaged for the problems we consider here so that surface approaches should be our focus.

Now that the issue of efficient and highly accurate enforcement of quasi-periodic boundary conditions has been largely resolved [20–27], an implementation in terms of IEs is compelling and we plan to investigate this in a future publication. However, we now focus upon geometries which are parametrized by a real number, ε, and thus choose to discuss HOPS schemes, more specifically the stable and high-order accurate TFE approach of Nicholls & Reitich [36,37,53–55]. To focus our developments and abbreviate the presentation, we consider only the operators $R(m)$ corresponding to inner layers. The upper and lower layer operators, Q and S, can be handled in a similar manner. Our developments follow §5 of [39] quite closely and we direct the interested reader there for more details.

To begin, we recall the defining boundary value problem (3.4) for the inner layer IIO, and the definition of the IIO itself (3.5). For brevity, we simplify the notation slightly,

$$\Delta v + k^2 v = 0, \quad -\bar{h} + \ell(x,y) < z < \bar{h} + u(x,y), \tag{5.1a}$$

$$\partial_z v - (\partial_x u)\partial_x v - (\partial_y u)\partial_y v - \mathrm{i}\eta v = U, \quad z = \bar{h} + u(x,y) \tag{5.1b}$$

and

$$-\partial_z v + (\partial_x \ell)\partial_x v + (\partial_y \ell)\partial_y v - \mathrm{i}\eta v = L, \quad z = -\bar{h} + \ell(x,y), \tag{5.1c}$$

where $v = v^{(m)}$, $k = k^{(m)}$, $\bar{h} = a^{(m)}$, $-\bar{h} = a^{(m+1)}$, $u = g^{(m)}$, $\ell = g^{(m+1)}$, and the IIO is given by

$$R[U,L] = \begin{pmatrix} R^{(u)}[U,L] \\ R^{(\ell)}[U,L] \end{pmatrix} = \begin{pmatrix} [\partial_z v - (\partial_x u)\partial_x v - (\partial_y u)\partial_y v + \mathrm{i}\eta v]_{z=\bar{h}+u} \\ [-\partial_z v + (\partial_x \ell)\partial_x v + (\partial_y \ell)\partial_y v + \mathrm{i}\eta v]_{z=-\bar{h}+\ell} \end{pmatrix},$$

where $R = R(m)$.

Following in the footsteps of Nicholls & Reitich [37,53,55], we introduce the following changes of variables (also known as σ-coordinates in the atmospheric sciences [56] and the C-method in electrodynamics [57]):

$$x' = x, \quad y' = y, \quad z' = -\bar{h}\left(\frac{\bar{h} + u(x,y) - z}{2\bar{h} + u(x,y) - \ell(x,y)}\right) + \bar{h}\left(\frac{z + \bar{h} - \ell(x,y)}{2\bar{h} + u(x,y) - \ell(x,y)}\right),$$

which maps the perturbed domain

$$S_{-\bar{h}+\ell,\bar{h}+u} = \{-\bar{h} + \ell(x,y) < z < \bar{h} + u(x,y)\}$$

to the flat-interface domain $S_{-\bar{h},\bar{h}}$, which has height $2\bar{h}$. The function $v = v(x,y,z)$ transforms to

$$w = w(x',y',z') = v(x(x',y',z'), y(x',y',z'), z(x',y',z')),$$

and it can be shown [39] that (5.1a) transforms to

$$\mathrm{div}'\,[A\nabla' w] + B \cdot \nabla' w + k^2 C^2 w = 0, \quad -\bar{h} < z' < \bar{h}, \tag{5.2}$$

where forms for A, B and C can be found in [39]; for ease of exposition, from here we drop the primed notation. If we set $u = \varepsilon\tilde{u}$ and $\ell = \delta\tilde{\ell}$, then

$$A = A(\varepsilon,\delta) = A_{0,0} + A_{1,0}\varepsilon + A_{0,1}\delta + A_{2,0}\varepsilon^2 + A_{1,1}\varepsilon\delta + A_{0,2}\delta^2,$$

$$B = B(\varepsilon,\delta) = B_{1,0}\varepsilon + B_{0,1}\delta + B_{2,0}\varepsilon^2 + B_{1,1}\varepsilon\delta + B_{0,2}\delta^2$$

and

$$C^2 = C^2(\varepsilon,\delta) = C^2_{0,0} + C^2_{1,0}\varepsilon + C^2_{0,1}\delta + C^2_{2,0}\varepsilon^2 + C^2_{1,1}\varepsilon\delta + C^2_{0,2}\delta^2,$$

where the $A_{n,r}$, $B_{n,r}$ and $C_{n,r}$ are given in [39]. With these, we write (5.2) as

$$\Delta w + k^2 w = F, \quad -\bar{h} < z < \bar{h}, \tag{5.3}$$

where

$$F = \mathrm{div}\,[(I - A)\nabla w] - B \cdot \nabla w + k^2(1 - C^2)w,$$

and if $u = \varepsilon\tilde{u}$ and $\ell = \delta\tilde{\ell}$, then $F = \mathcal{O}(\varepsilon) + \mathcal{O}(\delta)$.

In our first departure from [39], we find that the boundary conditions (5.1b,c) transform to

$$\partial_z w - \mathrm{i}\eta w = U + J^{(u)}, \quad z = \bar{h} \tag{5.4a}$$

and

$$-\partial_z w - \mathrm{i}\eta w = L + J^{(\ell)}, \quad z = -\bar{h}, \tag{5.4b}$$

where

$$2\bar{h}J^{(u)} = uU - \ell U + (\mathrm{i}\eta)uw - (\mathrm{i}\eta)\ell w + 2\bar{h}(\partial_x u)\partial_x w + u(\partial_x u)\partial_x w - \ell(\partial_x u)\partial_x w - 2\bar{h}(\partial_x u)^2\partial_z w$$

and

$$2\bar{h}J^{(\ell)} = uU - \ell U + (\mathrm{i}\eta)uw - (\mathrm{i}\eta)\ell w - 2\bar{h}(\partial_x u)\partial_x w - u(\partial_x \ell)\partial_x w + \ell(\partial_x \ell)\partial_x w + 2\bar{h}(\partial_x \ell)^2\partial_z w,$$

and $J = \mathcal{O}(\varepsilon) + \mathcal{O}(\delta)$ if $u = \varepsilon\tilde{u}$ and $\ell = \delta\tilde{\ell}$.

We close by noting that the IIO

$$\begin{pmatrix} R^{(u)}[U,L] \\ R^{(\ell)}[U,L] \end{pmatrix} = \begin{pmatrix} [\partial_z v - (\partial_x u)\partial_x v - (\partial_y u)\partial_y v + \mathrm{i}\eta v]_{z=\bar{h}+u} \\ [-\partial_z v + (\partial_x \ell)\partial_x v + (\partial_y \ell)\partial_y v + \mathrm{i}\eta v]_{z=-\bar{h}+\ell} \end{pmatrix}$$

transforms (upon dropping primes) to

$$\begin{pmatrix} R^{(u)}[U,L] \\ R^{(\ell)}[U,L] \end{pmatrix} = \begin{pmatrix} [\partial_z w + \mathrm{i}\eta w]_{z=\bar{h}} \\ [-\partial_z w + \mathrm{i}\eta w]_{z=-\bar{h}} \end{pmatrix} + \begin{pmatrix} K^{(u)} \\ K^{(\ell)} \end{pmatrix}, \tag{5.5}$$

where

$$2\bar{h}K^{(u)} = -(\partial_x u)\partial_x w + (\mathrm{i}\eta)uw - (\mathrm{i}\eta)\ell w - uK^{(u)} + \ell K^{(u)} - u(\partial_x u)\partial_x w + \ell(\partial_x u)\partial_x w + (\partial_x u)^2\partial_z w$$

and

$$2\bar{h}K^{(\ell)} = (\partial_x \ell)\partial_x w + (\mathrm{i}\eta)uw - (\mathrm{i}\eta)\ell w - uK^{(\ell)} + \ell K^{(\ell)} + u(\partial_x \ell)\partial_x w - \ell(\partial_x \ell)\partial_x w - (\partial_x \ell)^2\partial_z w,$$

and again, if $u = \varepsilon\tilde{u}$ and $\ell = \delta\tilde{\ell}$, then $\{K^{(u)}, K^{(\ell)}\} = \mathcal{O}(\delta) + \mathcal{O}(\varepsilon)$.

We now gather our field equations in transformed coordinates

$$\Delta w + k^2 w = F, \quad -\bar{h} < z < \bar{h}, \tag{5.6a}$$

$$\partial_z w - \mathrm{i}\eta w = U + J^{(u)}, \quad z = \bar{h} \tag{5.6b}$$

and

$$-\partial_z w - \mathrm{i}\eta w = L + J^{(\ell)}, \quad z = -\bar{h}, \tag{5.6c}$$

cf. (5.3) and (5.4), together with the transformed equation for the IIO

$$\begin{pmatrix} R^{(u)}[U,L] \\ R^{(\ell)}[U,L] \end{pmatrix} = \begin{pmatrix} [\partial_z w + \mathrm{i}\eta w]_{z=\bar{h}} \\ [-\partial_z w + \mathrm{i}\eta w]_{z=-\bar{h}} \end{pmatrix} + \begin{pmatrix} K^{(u)} \\ K^{(\ell)} \end{pmatrix}, \tag{5.7}$$

cf. (5.5). At this point, we make the specification that, for $\varepsilon, \delta \in \mathbf{R}$,

$$u = \varepsilon\tilde{u} \quad \text{and} \quad \ell = \delta\tilde{\ell},$$

where the (implicit) smallness assumptions on ε and δ can be removed (up to topological obstruction [55]). With this, we can formally expand

$$w = w(x,y,z;\varepsilon,\delta) = \sum_{n=0}^{\infty}\sum_{r=0}^{\infty} w_{n,r}(x,y,z)\varepsilon^n\delta^r$$

and

$$R = \begin{pmatrix} R^{(u)} \\ R^{(\ell)} \end{pmatrix} = \begin{pmatrix} R^{(u)}(x,y;\varepsilon,\delta) \\ R^{(\ell)}(x,y;\varepsilon,\delta) \end{pmatrix} = \sum_{n=0}^{\infty}\sum_{r=0}^{\infty} \begin{pmatrix} R^{(u)}_{n,r}(x,y) \\ R^{(\ell)}_{n,r}(x,y) \end{pmatrix} \varepsilon^n\delta^r,$$

and find that, at each perturbation order $\mathcal{O}(\varepsilon^n\delta^r)$, we must solve

$$\Delta w_{n,r} + k^2 w_{n,r} = F_{n,r}, \quad -\bar{h} < z < \bar{h},$$
$$\partial_z w_{n,r} - \mathrm{i}\eta w_{n,r} = U_{n,r} + J^{(u)}_{n,r}, \quad z = \bar{h}$$

and

$$-\partial_z w_{n,r} - \mathrm{i}\eta w_{n,r} = L_{n,r} + J^{(\ell)}_{n,r}, \quad z = -\bar{h},$$

where

$$\begin{pmatrix} R^{(u)}_{n,r}[U,L] \\ R^{(\ell)}_{n,r}[U,L] \end{pmatrix} = \begin{pmatrix} [\partial_z w_{n,r} + \mathrm{i}\eta w_{n,r}]_{z=\bar{h}} \\ [-\partial_z w_{n,r} + \mathrm{i}\eta w_{n,r}]_{z=-\bar{h}} \end{pmatrix} + \begin{pmatrix} K^{(u)}_{n,r} \\ K^{(\ell)}_{n,r} \end{pmatrix}.$$

In these

$$F_{n,r} = -\sum_{\nu+\rho=1}^{2} \{\mathrm{div}\left[A_{\nu,\rho}\nabla w_{n-\nu,r-\rho}\right] + B_{\nu,\rho}\cdot\nabla w_{n-\nu,r-\rho} + k^2 C^2_{\nu,\rho} w_{n-\nu,r-\rho}\},$$

$$\begin{aligned} 2\bar{h}J^{(u)}_{n,r} &= \tilde{u}U_{n-1,r} - \tilde{\ell}U_{n,r-1} + (\mathrm{i}\eta)\tilde{u}w_{n-1,r} - (\mathrm{i}\eta)\tilde{\ell}w_{n,r-1} + 2\bar{h}(\partial_x\tilde{u})\partial_x w_{n-1,r} \\ &\quad + \tilde{u}(\partial_x\tilde{u})\partial_x w_{n-2,r} - \tilde{\ell}(\partial_x\tilde{u})\partial_x w_{n-1,r-1} - 2\bar{h}(\partial_x\tilde{u})^2\partial_z w_{n-2,r}, \\ 2\bar{h}J^{(\ell)}_{n,r} &= \tilde{u}U_{n-1,r} - \tilde{\ell}U_{n,r-1} + (\mathrm{i}\eta)\tilde{u}w_{n-1,r} - (\mathrm{i}\eta)\tilde{\ell}w_{n,r-1} - 2\bar{h}(\partial_x\tilde{u})\partial_x w_{n-1,r} \\ &\quad - \tilde{u}(\partial_x\tilde{\ell})\partial_x w_{n-1,r-1} + \tilde{\ell}(\partial_x\tilde{\ell})\partial_x w_{n,r-2} + 2\bar{h}(\partial_x\tilde{\ell})^2\partial_z w_{n,r-2}, \\ 2\bar{h}K^{(u)}_{n,r} &= -(\partial_x\tilde{u})\partial_x w_{n-1,r} + (\mathrm{i}\eta)\tilde{u}w_{n-1,r} - (\mathrm{i}\eta)\tilde{\ell}w_{n,r-1} - \tilde{u}K^{(u)}_{n-1,r} + \tilde{\ell}K^{(u)}_{n,r-1} \\ &\quad - \tilde{u}(\partial_x\tilde{u})\partial_x w_{n-2,r} + \tilde{\ell}(\partial_x\tilde{u})\partial_x w_{n-1,r-1} + (\partial_x\tilde{u})^2\partial_z w_{n-2,r} \end{aligned}$$

and

$$\begin{aligned} 2\bar{h}K^{(\ell)}_{n,r} &= (\partial_x\tilde{\ell})\partial_x w_{n,r-1} + (\mathrm{i}\eta)\tilde{u}w_{n-1,r} - (\mathrm{i}\eta)\tilde{\ell}w_{n,r-1} - \tilde{u}K^{(\ell)}_{n-1,r} + \tilde{\ell}K^{(\ell)}_{n,r-1} \\ &\quad + \tilde{u}(\partial_x\tilde{\ell})\partial_x w_{n-1,r-1} - \tilde{\ell}(\partial_x\tilde{\ell})\partial_x w_{n,r-2} - (\partial_x\tilde{\ell})^2\partial_z w_{n,r-2}. \end{aligned}$$

6. Numerical results

In this section, we describe a variety of numerical experiments we conducted with our DNO and IIO formulations of the layered medium problems we consider here, and report on the results of these. We began by demonstrating the validity of our algorithm by conducting experiments using the method of manufactured solutions (MMS) [58,59]. We then showed comparisons between TFE simulations of a three-layer configuration with the DNO formulation [45] and our new IIO version (3.8). More specifically, we considered a configuration far from singularities of the inner-layer DNO, H, and a structure exactly (up to machine precision) at a singularity. We concluded with the simulation of the reflectivity map of a triply layered dielectric–metal–dielectric (DMD) structure.

Our numerical approach to solving the layered medium problems presented in this section is to use either the DNO formulation of the problem [45] or its IIO counterpart (3.8), with the relevant operators (DNOs and IIOs, respectively) simulated using the TFE methodology. For brevity, we discuss how this is accomplished for the interior layer IIO, R, described in detail in §5.

We recall from (3.4) that inputs to the IIO, given in (3.5), are the impedance data $\{U^{(m),u}, U^{(m),\ell}\}$ and the boundary deformations $\{g^{(m)}, g^{(m+1)}\}$ with half-layer thickness $\bar{h}^{(m)} := (a^{(m)} - a^{(m+1)})/2$. We sought a solution of the field equations (5.6) in the form

$$w^{(N_x,N_y,N_z,N)}(x,y,z;\varepsilon,\delta) = \sum_{n=0}^{N}\sum_{r=0}^{N}\sum_{p=-N_x/2}^{N_x/2-1}\sum_{q=-N_y/2}^{N_y/2-1}\sum_{\ell=0}^{N_z} \hat{w}_{p,q,\ell,n,r} \times T_\ell\left(\frac{2z - a^{(m+1)} - a^{(m)}}{a^{(m)} - a^{(m+1)}}\right) \mathrm{e}^{\mathrm{i}\alpha_p x + \mathrm{i}\beta_q y}\varepsilon^n\delta^r,$$

where T_ℓ is the ℓth Chebyshev polynomial, and the solution of the IIO problem (5.7) of the type

$$R^{(N_x,N_y,N_z,N)}(\varepsilon,\delta)=\sum_{n=0}^{N}\sum_{r=0}^{N}R_{n,r}\varepsilon^n\delta^r.$$

While one could pursue these *joint* Taylor series expansions with independent choices of ε and δ, we have not found such an approach to be competitive in terms of operation counts. Instead, we chose to study the special case of $\varepsilon=\delta$, which, of course, still permits one to study the perturbed geometry setting which we set as our goal at the outset.

An important question is how the Taylor series in ε are summed, for instance the truncation $R^{(N_x,N_y,N_z,N)}$ of R. This particular approximation distils to simulating $r_{p,q}(\varepsilon):=\sum_{n=0}^{\infty}r_{p,q,n}\varepsilon^n$ by $r^N_{p,q}(\varepsilon):=\sum_{n=0}^{N}r_{p,q,n}\varepsilon^n$. For this task, the classical analytic continuation technique of Padé approximation [60] has been used with HOPS methods with great success [33,55] and we advocate its use here. Padé approximation seeks to estimate the truncated Taylor series $r^N_{p,q}(\varepsilon)$ by the rational function

$$\left[\frac{L}{M}\right](\varepsilon):=\frac{a^L(\varepsilon)}{b^M(\varepsilon)}=\frac{\sum_{\ell=0}^{L}a_\ell\varepsilon^\ell}{1+\sum_{m=1}^{M}b_m\varepsilon^m},\quad L+M=N$$

and

$$\left[\frac{L}{M}\right](\varepsilon)=r^N_{p,q}(\varepsilon)+\mathcal{O}(\varepsilon^{L+M+1});$$

well-known formulae for the coefficients $\{a_\ell,b_m\}$ can be found in [60]. This approximant has remarkable properties of enhanced convergence, and we refer the interested reader to §2.2 of Baker & Graves–Morris [60] and the insightful calculations of §8.3 of Bender & Orszag [61] for a thorough discussion of the capabilities and limitations of Padé approximants.

(a) Validation by the method of manufactured solutions

Regarding the MMS, we focused upon the three-layer problem with layers $m=0,1,2$ denoted, for simplicity, by the letters $\{u,v,w\}$, respectively. Consider the quasi-periodic, outgoing solutions of the Helmholtz equation (3.2*a*)

$$u_{r,s}(x,y,z):=A^u_{r,s}\,\mathrm{e}^{\mathrm{i}\alpha_r x+\mathrm{i}\beta_s y+\mathrm{i}\gamma^u_{r,s}z},\quad r,s\in\mathbf{Z},\quad A^u_{r,s}\in\mathbf{C},$$

and their counterparts for (3.6*a*)

$$w_{r,s}(x,y,z):=A^w_{r,s}\,\mathrm{e}^{\mathrm{i}\alpha_r x+\mathrm{i}\beta_s y-\mathrm{i}\gamma^w_{r,s}z},\quad r,s\in\mathbf{Z},\quad A^w_{r,s}\in\mathbf{C}.$$

Further, consider the quasi-periodic solutions of the Helmholtz equation (3.4*a*)

$$v_{r,s}(x,y,z):=A^v_{r,s}\,\mathrm{e}^{\mathrm{i}\alpha_r x+\mathrm{i}\beta_s y+\mathrm{i}\gamma^v_{r,s}z}+B^v_{r,s}\,\mathrm{e}^{\mathrm{i}\alpha_r x+\mathrm{i}\beta_s y-\mathrm{i}\gamma^v_{r,s}z},\quad r,s\in\mathbf{Z},\ A^v_{r,s},B^v_{r,s}\in\mathbf{C}.$$

We selected two simple sinusoidal profiles

$$\left.\begin{aligned}g^u(x,y)&=\varepsilon f^u(x,y)=\varepsilon\cos(2x-3y)\\ \text{and}\qquad g^\ell(x,y)&=\varepsilon f^\ell(x,y)=\varepsilon\sin(3x-2y),\end{aligned}\right\}\tag{6.1}$$

and defined, for any choice of the layer half-thickness $\bar h$, the Dirichlet and Neumann traces

$$\begin{aligned}&\xi^u_{r,s}(x,y):=u_{r,s}(x,y,\bar h+g^u(x,y)),\quad v^u_{r,s}(x,y):=(-\partial_{N^u}u_{r,s})(x,y,\bar h+g^u(x,y)),\\ &\xi^w_{r,s}(x,y):=w_{r,s}(x,y,-\bar h+g^\ell(x,y)),\quad v^w_{r,s}(x,y):=(\partial_{N^\ell}w_{r,s})(x,y,-\bar h+g^\ell(x,y)),\\ &\xi^v_{r,s}(x,y):=v_{r,s}(x,y,\bar h+g^u(x,y)),\quad v^v_{r,s}(x,y):=(\partial_{N^u}v_{r,s})(x,y,\bar h+g^u(x,y))\\ \text{and}\qquad &\zeta^v_{r,s}(x,y):=v_{r,s}(x,y,-\bar h+g^\ell(x,y)),\quad \psi^v_{r,s}(x,y):=(-\partial_{N^\ell}v_{r,s})(x,y,-\bar h+g^\ell(x,y)).\end{aligned}$$

From these, we defined, for any real $\eta > 0$, the impedances

$$U_{r,s} := \nu^u_{r,s} - \mathrm{i}\eta\xi^u_{r,s}, \quad \tilde{U}_{r,s} := \nu^u_{r,s} + \mathrm{i}\eta\xi^u_{r,s}, \quad W_{r,s} := \nu^w_{r,s} - \mathrm{i}\eta\xi^w_{r,s},$$
$$\tilde{W}_{r,s} := \nu^w_{r,s} + \mathrm{i}\eta\xi^w_{r,s}, \quad V^u_{r,s} := \nu^v_{r,s} - \mathrm{i}\eta\xi^v_{r,s}, \quad \tilde{V}^u_{r,s} := \nu^v_{r,s} + \mathrm{i}\eta\xi^v_{r,s}$$
and
$$V^\ell_{r,s} := \psi^v_{r,s} - \mathrm{i}\eta\zeta^v_{r,s}, \quad \tilde{V}^\ell_{r,s} := \psi^v_{r,s} + \mathrm{i}\eta\zeta^v_{r,s}.$$

We chose the following physical parameters:

$$\left.\begin{aligned} &d_x = 2\pi, \quad d_y = 2\pi, \quad \alpha = 0.1, \quad \beta = 0.2, \quad \gamma_u = 1.21, \\ &\gamma_v = 1.97, \quad \gamma_w = 2.23, \quad A^u_{r,s} = -3\delta_{2,1}, \quad A^w_{r,s} = 4\delta_{3,1} \\ \text{and} \quad &B^v_{r,s} = -e\delta_{3,1}, \quad C^v_{r,s} = \pi\delta_{3,1}, \quad \eta \approx 1.7358 \end{aligned}\right\} \tag{6.2}$$

(where $\delta_{r,s}$ is the Kronecker delta) in TM polarization, and the numerical parameters

$$N_x = 64, \quad N_y = 64, \quad N_z = 32, \quad N = 10, \quad a = 1/2, \quad b = 1/2. \tag{6.3}$$

To elucidate the behaviour of our scheme, we studied four choices of $\varepsilon = 0.005, 0.01, 0.05, 0.1$; cf. (6.1). For this, we supplied $\{\xi^u_{r,s}, \xi^v_{r,s}, \zeta^v_{r,s}, \xi^w_{r,s}\}$ to our HOPS algorithm to simulate solutions of the DNO formulation of the three-layer scattering problem, $\{\nu^{u,\mathrm{approx}}_{r,s}, \nu^{v,\mathrm{approx}}_{r,s}, \psi^{v,\mathrm{approx}}_{r,s}, \nu^{w,\mathrm{approx}}_{r,s}\}$, and computed the relative error

$$\mathrm{Error}^{\mathrm{DNO}}_{\mathrm{rel}} := \frac{\left|\nu^u_{r,s} - \nu^{u,\mathrm{approx}}_{N_x,N_y,N_z,N}\right|_{L^\infty}}{\left|\nu^u_{r,s}\right|_{L^\infty}}.$$

In a similar way, we passed $\{U_{r,s}, V^u_{r,s}, V^\ell_{r,s}, W_{r,s}\}$ to our HOPS algorithm to simulate solutions of the IIO formulation of the three-layer scattering problem, $\{\tilde{U}^{\mathrm{approx}}_{r,s}, \tilde{V}^{u,\mathrm{approx}}_{r,s}, \tilde{V}^{\ell,\mathrm{approx}}_{r,s}, \tilde{W}^{\mathrm{approx}}_{r,s}\}$, and computed the relative error

$$\mathrm{Error}^{\mathrm{IIO}}_{\mathrm{rel}} := \frac{\left|\tilde{U}_{r,s} - \tilde{U}^{\mathrm{approx}}_{N_x,N_y,N_z,N}\right|_{L^\infty}}{\left|\tilde{U}_{r,s}\right|_{L^\infty}}.$$

We note that the choice to measure the defect in these upper-layer quantities, $\nu^u_{r,s}$ and $U_{r,s}$, was rather arbitrary. Measuring the mismatch in any of the other output quantities produced similar results.

To begin our study, with the choice $\bar{h} = 0.33$ we carried out these simulations with our IIO method (3.8) and report our results in figure 2*a*,*b*. We repeated this with our DNO approach [45] and display the outcomes in figure 3*a*,*b*. We see in this generic, non-resonant, configuration that both algorithms display a spectral rate of convergence as N is refined (up to the conditioning of the algorithm), which improves as ε is decreased.

Before proceeding, we note that the choice of half-height $\bar{h} = \pi/\gamma_v$ will induce a singularity in the interior DNO, H, resulting in a lack of uniqueness. To test the performance of our methods near this scenario, we selected

$$\bar{h} = \frac{\pi}{\gamma_v} + \tau.$$

With the same choices of geometrical, (6.1), physical, (6.2), and numerical, (6.3), parameters as before, we selected $\tau = 10^{-16}$ resulting in $\bar{h} = 1.5947170830405 \approx \pi/\gamma_v + 10^{-16}$. After running simulations with the IIO method (3.8), we display our results in figure 4*a*,*b*. We revisited these computations with our DNO approach [45] and show our results in figure 5*a*,*b*. We see in this resonant (to machine precision) configuration, the IIO algorithm again displays a spectral rate of convergence as N is refined (improving as ε is decreased), while the DNO approach delivers completely unacceptable results, even with Padé approximation.

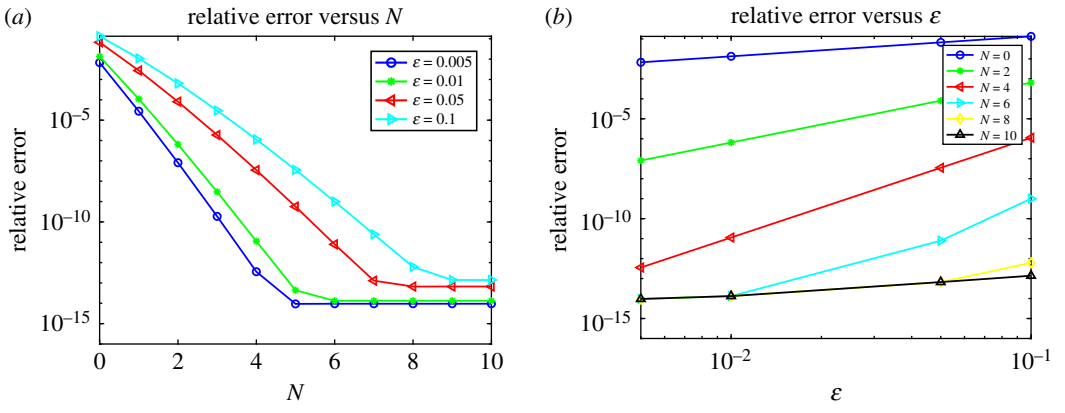

Figure 2. Plot of relative error with six choices of $N = 0, 2, 4, 6, 8, 10$ for a non-resonant configuration using the IIO formulation with Taylor summation. (*a*) Error versus perturbation order, N. (*b*) Error versus perturbation size, ε. (Online version in colour.)

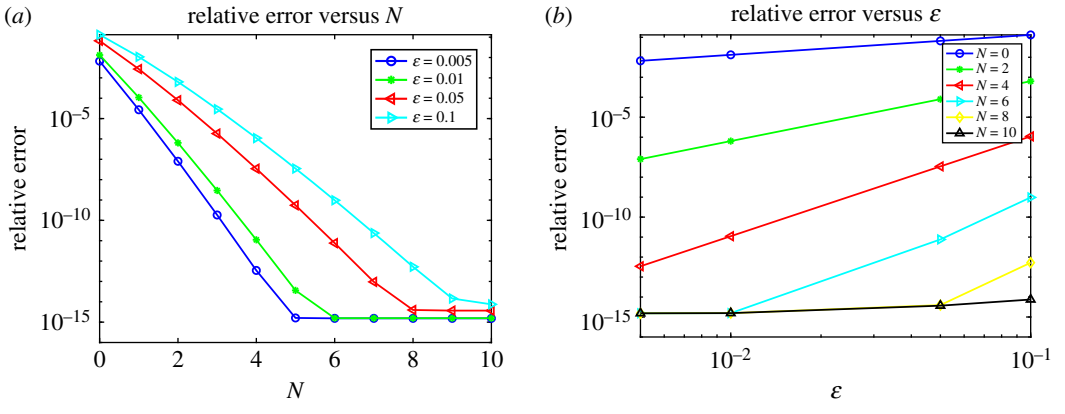

Figure 3. Plot of relative error with six choices of $N = 0, 2, 4, 6, 8, 10$ for a non-resonant configuration using the DNO formulation with Taylor summation. (*a*) Error versus perturbation order, N. (*b*) Error versus perturbation size, ε. (Online version in colour.)

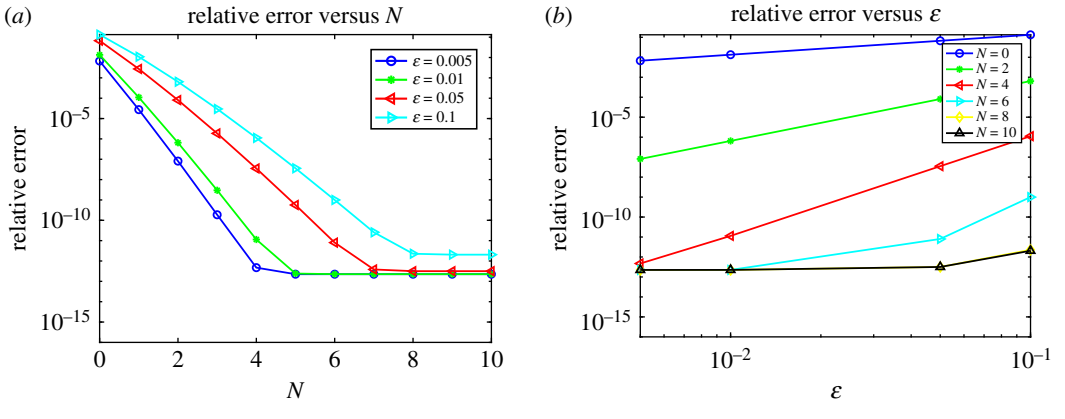

Figure 4. Plot of relative error with six choices of $N = 0, 2, 4, 6, 8, 10$ for a resonant configuration using the IIO formulation with Taylor summation. (*a*) Error versus perturbation order, N. (*b*) Error versus perturbation size, ε. (Online version in colour.)

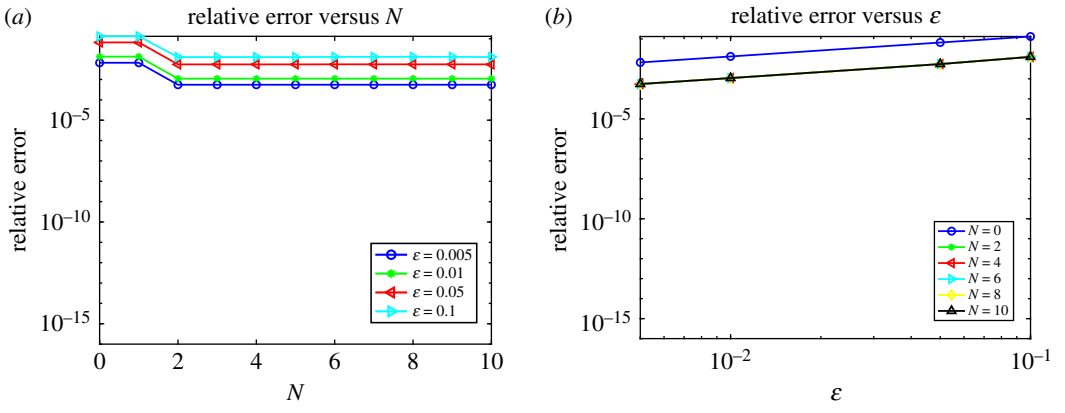

Figure 5. Plot of relative error with six choices of $N = 0, 2, 4, 6, 8, 10$ for a resonant configuration using the DNO formulation with Padé summation. (*a*) Error versus perturbation order, N. (*b*) Error versus perturbation size, ε. (Online version in colour.)

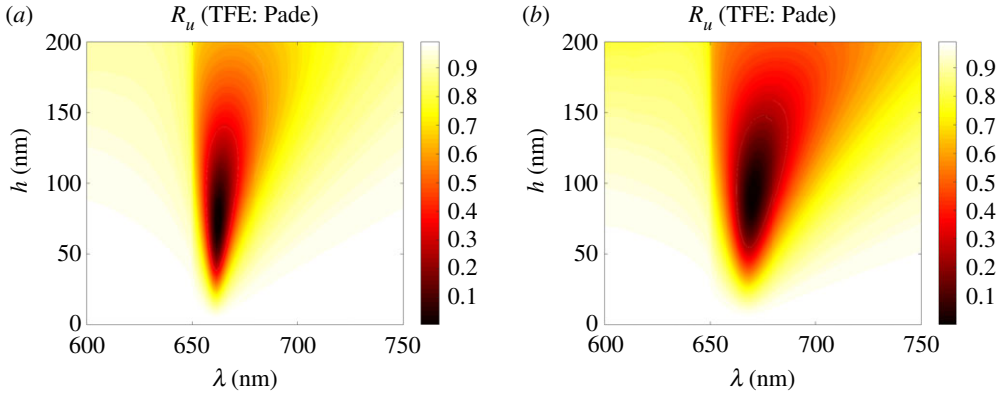

Figure 6. Reflectivity map for three layers, $R(\lambda, h)$, versus incident wavelength, λ, and deformation height, h. Results for gold layer thickness $2\bar{h} = 25, 50$ nm and the double sinusoid configuration, (6.4) and (6.5), with $N_x = N_y = 24$, $N_z = 32$, [8/8] Padé approximant. (*a*) $2\bar{h} = 100$ nm and (*b*) $2\bar{h} = 50$ nm. (Online version in colour.)

(b) Simulation of triply layered structures

In conclusion, we considered a structure similar to one constructed in the laboratory of S.–H. Oh (Minnesota), in particular the DMD devices described in [7,44]. Such a simulation required a slight generalization of our developments to accommodate a single lossy layer (the metal) characterized by a permittivity with non-zero imaginary part, but this posed no significant difficulties. A *two-dimensional* thin-film sensor was built which was corrugated on one side and *flat* on the other. With our new code, we can investigate such structures, which feature corrugations on *both* sides. While not addressing the full vector Maxwell equations, we performed these simulations in three dimensions for the scalar Helmholtz equations. The Maxwell case is the subject of current investigations.

For definiteness, we considered a three-layer configuration consisting of vacuum (a dielectric) overlaying a *thin* layer of gold (a metal) of thickness $2\bar{h}$ on top of water (a dielectric) with interfaces shaped by $g^{(m)} = hf^{(m)}$

$$f^{(1)}(x,y) = f^{(2)}(x,y) = \frac{1}{4}\left\{\cos\left(\frac{2\pi x}{d_x}\right) + \cos\left(\frac{2\pi y}{d_y}\right)\right\}. \tag{6.4}$$

By definition, the refractive index for vacuum is $n^{\text{vac}} = 1$ and for the refractive index of water we used the value $n^{\text{water}} = 1.333$ [7]. The refractive index of gold is the subject of ongoing research and we chose a Lorentz model [62]. We investigated two values of the half-height, $\bar{h} = 25, 50$ nm, and for physical and numerical parameters we selected the following:

$$\alpha = 0, \quad \beta = 0, \quad \gamma^{(0)} = \gamma^{\text{vac}}, \quad \gamma^{(1)} = \gamma^{\text{Au}}, \quad \gamma^{(2)} = \gamma^{\text{water}}, \tag{6.5a}$$

$$h = 0, \ldots, 200\,\text{nm}, \quad d_x = d_y = 650\,\text{nm} \tag{6.5b}$$

and

$$N_x = N_y = 24, \quad N_z = 32, \quad N = 0, \ldots, 16. \tag{6.5c}$$

We point out the completely different *qualitative* character of the reflectivity maps for the $\bar{h} = 50$ nm (figure 6*a*) and $\bar{h} = 25$ nm (figure 6*b*) cases; the region of sensitive response is vastly enlarged in the latter case. One factor for this difference is the fact that the thin-layer configuration allows radiation to transmit into the water as its vertical dimension is now comparable to the skin depth of gold. A central conclusion of this contribution is that our new methodology permits very rapid and reliable simulation of system parameters for configurations like these.

Data accessibility. Relevant MATLAB code can be found at: https://github.com/dpnicholls71/IIOStabPaper.

Competing interests. I declare I have no competing interests.

Funding. This work was supported by National Science Foundation grant no. DMS–1522548.

Acknowledgements. D.P.N. gratefully acknowledges support from the National Science Foundation through grant no. DMS–1522548. He also thanks A. Barnett for helpful hints and comments during the preparation of this manuscript.

References

1. Tsang L, Kong JA, Shin RT. 1985 *Theory of microwave remote sensing*. New York, NY: Wiley.
2. Shull PJ. 2002 *Nondestructive evaluation: theory, techniques, and applications*. New York, NY: Marcel Dekker.
3. Brekhovskikh LM, Lysanov YP. 1982 *Fundamentals of ocean acoustics*. Berlin, Germany: Springer.
4. Ebbesen TW, Lezec HJ, Ghaemi HF, Thio T, Wolff PA. 1998 Extraordinary optical transmission through sub-wavelength hole arrays. *Nature* **391**, 667–669. (doi:10.1038/35570)
5. Moskovits M. 1985 Surface-enhanced spectroscopy. *Rev. Mod. Phys.* **57**, 783–826. (doi:10.1103/RevModPhys.57.783)
6. Homola J. 2008 Surface plasmon resonance sensors for detection of chemical and biological species. *Chem. Rev.* **108**, 462–493. (doi:10.1021/cr068107d)
7. Lindquist NC, Johnson TW, Jose J, Otto LM, Oh SH. 2012 Ultrasmooth metallic films with buried nanostructures for backside reflection-mode plasmonic biosensing. *Ann. Phys.* **524**, 687–696. (doi:10.1002/andp.201200144)
8. Virieux J, Operto S. 2009 An overview of full-waveform inversion in exploration geophysics. *Geophysics* **74**, WCC1–WCC26. (doi:10.1190/1.3238367)
9. Geli L, Bard PY, Jullien B. 1988 The effect of topography on earthquake ground motion: a review and new results. *Bull. Seismol. Soc. Am.* **78**, 42–63.
10. Raether H. 1988 *Surface plasmons on smooth and rough surfaces and on gratings*. Berlin, Germany: Springer.
11. Deville MO, Fischer PF, Mund EH. 2002 *High-order methods for incompressible fluid flow*. Cambridge Monographs on Applied and Computational Mathematics, vol. 9. Cambridge, UK: Cambridge University Press.
12. Shen J, Tang T, Wang LL. 2011 *Spectral methods: algorithms, analysis and applications*. Springer Series in Computational Mathematics, vol. 41. Heidelberg, Germany: Springer.
13. LeVeque RJ. 2007 *Finite difference methods for ordinary and partial differential equations: steady-state and time-dependent problems*. Philadelphia, PA: Society for Industrial and Applied Mathematics (SIAM).
14. Johnson C. 1987 *Numerical solution of partial differential equations by the finite element method*. Cambridge, UK: Cambridge University Press.
15. Hesthaven JS, Warburton T. 2008 *Nodal discontinuous Galerkin methods: algorithms, analysis, and applications*. Texts in Applied Mathematics, vol. 54. New York, NY: Springer.

16. Gottlieb D, Orszag SA. 1977 *Numerical analysis of spectral methods: theory and applications*. CBMS-NSF Regional Conference Series in Applied Mathematics, no. 26. Philadelphia, PA: Society for Industrial and Applied Mathematics.
17. Colton D, Kress R. 1998 *Inverse acoustic and electromagnetic scattering theory*, 2nd edn. Berlin, Germany: Springer.
18. Reitich F, Tamma K. 2004 State-of-the-art, trends, and directions in computational electromagnetics. *CMES Comput. Model. Eng. Sci.* **5**, 287–294.
19. Greengard L, Rokhlin V. 1987 A fast algorithm for particle simulations. *J. Comput. Phys.* **73**, 325–348. (doi:10.1016/0021-9991(87)90140-9)
20. Barnett A, Greengard L. 2011 A new integral representation for quasi-periodic scattering problems in two dimensions. *BIT Numer. Math.* **51**, 67–90. (doi:10.1007/s10543-010-0297-x)
21. Bruno O, Delourme B. 2014 Rapidly convergent two-dimensional quasi-periodic Green function throughout the spectrum—including Wood anomalies. *J. Comput. Phys.* **262**, 262–290. (doi:10.1016/j.jcp.2013.12.047)
22. Lai J, Kobayashi M, Barnett A. 2015 A fast and robust solver for the scattering from a layered periodic structure containing multi-particle inclusions. *J. Comput. Phys.* **298**, 194–208. (doi:10.1016/j.jcp.2015.06.005)
23. Cho MH, Barnett AH. 2015 Robust fast direct integral equation solver for quasi-periodic scattering problems with a large number of layers. *Opt. Express* **23**, 1775–1799. (doi:10.1364/OE.23.001775)
24. Bruno OP, Lyon M, Pérez-Arancibia C, Turc C. 2016 Windowed Green function method for layered-media scattering. *SIAM J. Appl. Math.* **76**, 1871–1898. (doi:10.1137/15M1033782)
25. Bruno OP, Shipman SP, Turc C, Venakides S. 2016 Superalgebraically convergent smoothly windowed lattice sums for doubly periodic Green functions in three-dimensional space. *Proc. R. Soc. A* **472**, 20160255. (doi:10.1098/rspa.2016.0255)
26. Bruno OP, Fernandez-Lado AG. 2017 Rapidly convergent quasi-periodic Green functions for scattering by arrays of cylinders—including Wood anomalies. *Proc. R. Soc. A* **473**, 20160802. (doi:10.1098/rspa.2016.0802)
27. Bruno OP, Pérez-Arancibia C. 2017 Windowed Green function method for the Helmholtz equation in the presence of multiply layered media. *Proc. R. Soc. A* **473**, 20170161. (doi:10.1098/rspa.2017.0161)
28. Nicholls DP. 2015 Method of field expansions for vector electromagnetic scattering by layered periodic crossed gratings. *J. Opt. Soc. Am. A* **32**, 701–709. (doi:10.1364/JOSAA.32.000701)
29. Nicholls DP, Oh SH, Johnson TW, Reitich F. 2016 Launching surface plasmon waves via vanishingly small periodic gratings. *J. Opt. Soc. Am. A* **33**, 276–285. (doi:10.1364/JOSAA.33.000276)
30. Rayleigh L. 1907 On the dynamical theory of gratings. *Proc. R. Soc. Lond. A* **79**, 399–416. (doi:10.1098/rspa.1907.0051)
31. Rice SO. 1951 Reflection of electromagnetic waves from slightly rough surfaces. *Commun. Pure Appl. Math.* **4**, 351–378. (doi:10.1002/cpa.3160040206)
32. Bruno OP, Reitich F. 1993 Numerical solution of diffraction problems: a method of variation of boundaries. *J. Opt. Soc. Am. A* **10**, 1168–1175. (doi:10.1364/JOSAA.10.001168)
33. Bruno OP, Reitich F. 1993 Numerical solution of diffraction problems: a method of variation of boundaries. II. Finitely conducting gratings, Padé approximants, and singularities. *J. Opt. Soc. Am. A* **10**, 2307–2316. (doi:10.1364/JOSAA.10.002307)
34. Bruno OP, Reitich F. 1993 Numerical solution of diffraction problems: a method of variation of boundaries. III. Doubly periodic gratings. *J. Opt. Soc. Am. A* **10**, 2551–2562. (doi:10.1364/JOSAA.10.002551)
35. Bruno OP, Reitich F. 1998 Boundary-variation solutions for bounded-obstacle scattering problems in three dimensions. *J. Acoust. Soc. Am.* **104**, 2579–2583. (doi:10.1121/1.423840)
36. Nicholls DP, Reitich F. 2004 Shape deformations in rough-surface scattering: cancellations, conditioning, and convergence. *J. Opt. Soc. Am. A* **21**, 590–605. (doi:10.1364/JOSAA.21.000590)
37. Nicholls DP, Reitich F. 2004 Shape deformations in rough-surface scattering: improved algorithms. *J. Opt. Soc. Am. A* **21**, 606–621. (doi:10.1364/JOSAA.21.000606)
38. Gillman A, Barnett AH, Martinsson PG. 2015 A spectrally accurate direct solution technique for frequency-domain scattering problems with variable media. *BIT Numer. Math.* **55**, 141–170. (doi:10.1007/s10543-014-0499-8)
39. Nicholls DP. 2017 On analyticity of linear waves scattered by a layered medium. *J. Differ. Equ.* **263**, 5042–5089. (doi:10.1016/j.jde.2017.06.012)

40. Lions PL. 1990 On the Schwarz alternating method. III. A variant for nonoverlapping subdomains. In *Third Int. Symp. on Domain Decomposition Methods for Partial Differential Equations (Houston, TX, 1989)*, pp. 202–223. Philadelphia, PA: SIAM.
41. Després B. 1991 Méthodes de décomposition de domaine pour les problèmes de propagation d'ondes en régime harmonique. Le théorème de Borg pour l'équation de Hill vectorielle. Institut National de Recherche en Informatique et en Automatique (INRIA), Rocquencourt. Thèse, Université de Paris IX (Dauphine), Paris, France.
42. Després B. 1991 Domain decomposition method and the Helmholtz problem. In *Mathematical and numerical aspects of wave propagation phenomena* (*Strasbourg, 1991*) (eds G Cohen, L Halpern, P Joly), pp. 44–52. Philadelphia, PA: SIAM.
43. Collino F, Ghanemi S, Joly P. 2000 Domain decomposition method for harmonic wave propagation: a general presentation. *Comput. Methods Appl. Mech. Eng.* **184**, 171–211. (doi:10.1016/S0045-7825(99)00228-5)
44. Nicholls DP, Reitich F, Johnson TW, Oh SH. 2014 Fast high-order perturbation of surfaces (HOPS) methods for simulation of multi-layer plasmonic devices and metamaterials. *J. Opt. Soc. Am. A* **31**, 1820–1831. (doi:10.1364/JOSAA.31.001820)
45. Nicholls DP. 2012 Three-dimensional acoustic scattering by layered media: a novel surface formulation with operator expansions implementation. *Proc. R. Soc. A* **468**, 731–758. (doi:10.1098/rspa.2011.0555)
46. Achenbach JD. 1973 *Wave propagation in elastic solids*. Amsterdam, The Netherlands: North–Holland.
47. Petit R (ed.). 1980 *Electromagnetic theory of gratings*. Berlin, Germany: Springer.
48. Arens T. 2009 *Scattering by biperiodic layered media: the integral equation approach*. Karlsruhe, Germany: Habilitationsschrift Karlsruhe Institute of Technology.
49. Kirsch A, Monk P. 1994 An analysis of the coupling of finite-element and Nyström methods in acoustic scattering. *IMA J. Numer. Anal.* **14**, 523–544. (doi:10.1093/imanum/14.4.523)
50. Evans LC. 2010 *Partial differential equations*, 2nd edn. Providence, RI: American Mathematical Society.
51. Coifman R, Meyer Y. 1985 Nonlinear harmonic analysis and analytic dependence. In *Pseudodifferential operators and applications* (*Notre Dame, Ind., 1984*) (ed. F Treves), pp. 71–78. Providence, RI: American Mathematical Society.
52. Hu B, Nicholls DP. 2005 Analyticity of Dirichlet–Neumann operators on Hölder and Lipschitz domains. *SIAM J. Math. Anal.* **37**, 302–320. (doi:10.1137/S0036141004444810)
53. Nicholls DP, Reitich F. 2001 A new approach to analyticity of Dirichlet-Neumann operators. *Proc. R. Soc. Edinburgh Sect. A* **131**, 1411–1433. (doi:10.1017/S0308210500001463)
54. Nicholls DP, Reitich F. 2001 Stability of high-order perturbative methods for the computation of Dirichlet-Neumann operators. *J. Comput. Phys.* **170**, 276–298. (doi:10.1006/jcph.2001.6737)
55. Nicholls DP, Reitich F. 2003 Analytic continuation of Dirichlet-Neumann operators. *Numer. Math.* **94**, 107–146. (doi:10.1007/s002110200399)
56. Phillips NA. 1957 A coordinate system having some special advantages for numerical forecasting. *J. Atmos. Sci.* **14**, 184–185. (doi:10.1175/1520-0469(1957)014<0184:ACSHSS>2.0.CO;2)
57. Chandezon J, Raoult G, Maystre D. 1980 A new theoretical method for diffraction gratings and its numerical application. *J. Opt.* **11**, 235–241. (doi:10.1088/0150-536X/11/4/005)
58. Roache PJ. 1998 *Verification and validation in computational science and engineering*. Albuquerque, NM: Hermosa Publishers.
59. Roache PJ. 2002 Code verification by the method of manufactured solutions. *J. Fluids Eng.* **124**, 4–10. (doi:10.1115/1.1436090)
60. Baker Jr GA, Graves-Morris P. 1996 *Padé approximants*, 2nd edn. Cambridge, UK: Cambridge University Press.
61. Bender CM, Orszag SA. 1978 *Advanced mathematical methods for scientists and engineers*. International Series in Pure and Applied Mathematics. New York, NY: McGraw-Hill Book Co.
62. Rakic A, Djurisic A, Elazar J, Majewski M. 1998 Optical properties of metallic films for vertical-cavity optoelectronic devices. *Appl. Opt.* **37**, 5271–5283. (doi:10.1364/AO.37.005271)